Tellus (1996), 48A, 593–606
Printed in UK – all rights reserved

TELLUS
ISSN 0280–6495

On the ice-ocean response to wind forcing

By ANDERS OMSTEDT[1,*], LEIF NYBERG[1] and MATTI LEPPÄRANTA[2], [1]*Swedish Meteorological and Hydrological Institute, S-601 76 Norrköping, Sweden;* [2]*Department of Geophysics, P.O. Box 4, Fabianinkatu 24 A, FIN-00014 University of Helsinki, Finland*

(Manuscript received 17 March 1995; in final form 15 November 1995)

ABSTRACT

The ice-ocean response to variable winds is analysed based upon two types of models. An analytical ice-ocean model with linear stress laws and forced by periodic winds is first derived. Secondly a numerical, vertically resolved ice-ocean model is introduced. In the numerical model, the ice-water stress law is calculated from a turbulence model and the wind stress is calculated on the basis of a square law formation. By comparing the ice-ocean stress law formulations, it is illustrated that the numerical model predicts an ice-ocean stress law that has a power slightly less than 2 compared to 1 for the analytical model. The numerical prediction is in good accordance with field observations and the slight deviation from 2 is due to wall effects close to the ice-water interface. It is then demonstrated that the ice-ocean response to variable winds could be well simulated by both models, but the analytical model did not capture the wind dependency properly (because of the linear approach). The ice and current factors are amplified at wind frequencies close to inertial ($\omega = -f$) and damped at high positive and negative frequencies. The maximum ice and current factors at a wind frequency equal to the inertial oscillation are shown to be dependent only on the friction coefficients. With the constants applied in the present study, the maximum ice drift and current speed are equal to 7.8% and 5.5% of the wind speed, respectively. These steady state values are however quite unrealistic as they would require a uniformly changing wind direction for many inertial periods.

1. Introduction

The response of sea ice drift to winds is well documented. From early studies with Fram in the Arctic Ocean pack ice, Nansen (1902) found that the surface ice drift deviated 20° to 40° to the right of the wind. Ekman (1905) derived analytical solutions for the vertical distribution of the ocean surface currents and explained the deviation to the right as being a consequence of the rotation of the earth. Ekman also examined the ocean response to variable winds and presented an analytical solution to frictional free oscillations of currents due to a sudden wind increase. Oscillations of this type are called inertial and have been observed both in the ocean (Gustafson and Kullenberg, 1936) and in the ice (McPhee, 1978, 1986). Pure inertial oscillation is a special case, in which there is a momentum balance between inertial and Coriolis accelerations. In the case of drifting sea ice, the momentum balance is due to air and water stresses, internal ice stress and surface pressure gradient (Hibler, 1986). When the ice interaction is weak (the free-drifting ice case), the problem becomes more simple, and a one-dimensional approach is possible. Several studies have started from this approach when analysing, for example, wind and surface currents (Price, 1981), wind and ice drift in a deep sea (Martinson and Wamser, 1990), wind and ice drift in a shallow sea (Overland et al., 1984) and wind and coupled ice-ocean response (Leppäranta and Omstedt, 1990). In general, different solutions to

* Corresponding author.

constant winds have been analysed. But not many results are available about the ice-ocean response to variable winds, including spin-up, spin-down and stationary solutions during transient wind forcing.

The purpose of the present study is to analyse the ice-water response in shallow seas to changing winds over a wide range of forcing conditions, expanding the earlier work by Leppäranta and Omstedt (1990). Effects of ice interaction are not dealt with, instead the ice is assumed to move freely. The approach is based upon theoretical considerations, and two types of models are applied. An analytical model with linear stresses and forced by winds is first derived and analysed. This model is then calibrated and compared with a vertically resolved numerical ice-ocean model. In the numerical model the stresses are calculated on the basis of a two-equation turbulence model and the wind stresses from a square law formulation. The problem considered is outlined in Fig. 1.

The basic equations are given in Section 2. In Sections 3 and 9, the analytical model is derived and analysed. Then, the numerical model is outlined. In Section 5, the analytical and numerical models are compared and the response to variable winds is discussed. The applicability of the theoretical findings is discussed in Section 6. Finally, a summary and some conclusions are given in Section 7.

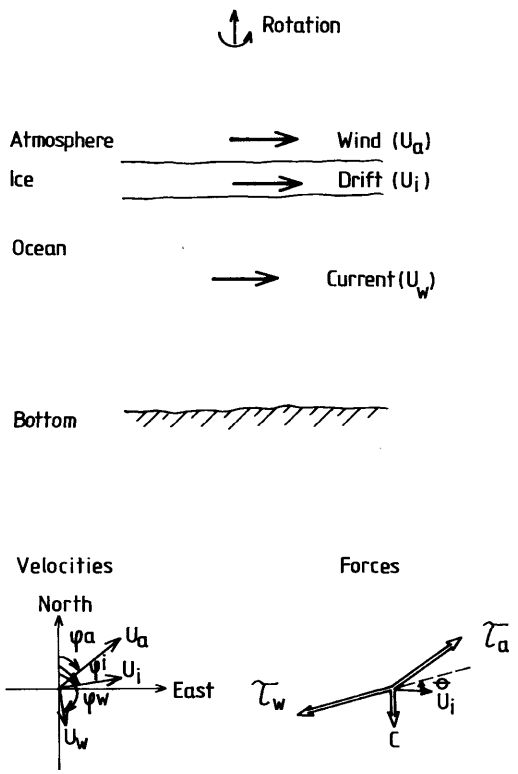

Fig. 1. Schematic figure for the problem considered. The wind, the ice drift and the current angles are denoted by ϕ^a, ϕ^i and ϕ^w respectively. All other notations are given in the text.

2. Basic equations

We consider the momentum conservation law of the ice-water system in a shallow sea, neglecting the lateral effects as well as interval waves. Then the system behaviour, forced by the air and bottom stresses, is determined by the internal and Coriolis accelerations and momentum transfer due to shear stress in the vertical.

We denote the velocity by U and the density by ρ using subscripts i for ice, w for water, a for air, b for bottom and the vertical shear stress by τ; the momentum equations in complex form then read:

$$\frac{\partial}{\partial t}(\rho_i U_i) + if\rho_i U_i = \frac{\partial \tau_i}{\partial z}, \tag{1}$$

$$\frac{\partial}{\partial t}(\rho_w U_w) + if\rho_w U_w = \frac{\partial \tau_w}{\partial z}, \tag{2}$$

where t is time, i is $\sqrt{-1}$, f is the Coriolis parameter and z is the vertical coordinate positive upward. The boundary conditions are:

$\tau = \tau_a$ at the ice upper surface,

$\tau = \tau_b$ at the bottom.

At the ice-water boundary, the interfacial ice-water shear stress (τ_0) couples the ice and the ocean. This stress reads:

$$\tau_0 = (\nu + \nu_T)\frac{\partial}{\partial z}\rho_w U_w, \tag{3}$$

where ν is the kinematic viscosity and ν_T the turbulent kinematic viscosity. In general $\nu_T \gg \nu$ and therefore molecular effects can be neglected. This will be the case in the present study. Eq. (1) is the time-dependent free ice drift equation, which

neglects the internal ice friction. Eq. (2) is the time-dependent Ekman equation.

To close the system, the interfacial shear stress needs to be determined. For simple assumptions about this stress (introducing linear bulk formulas), analytical models can be solved, this is done in Section 3. Using more advanced assumptions one needs to introduce turbulence models and solve the equations using numerical methods; this will be outlined in Section 4. A comparison of different interfacial stress laws are also given in Section 5.1.

Friction coefficients need to be determined in the stress formulations. In both the air-ice and the ice-water friction coefficients physical processes as skin and form drag are of importance. A prominent feature in the ice/water boundary layer is the large roughness elements which are due to ridged ice. Form drag may thus play an important role particularly at the ice-water interface. Drag coefficients under first-year ice, as in the Baltic Sea, are believed to be greater than under multi-year ice, as multi-year ice undergoes melting. A review on drag coefficients can be found in for example Shirasawa and Ingram (1991). In the present paper we apply friction coefficients from an earlier field study from the Baltic Sea (Leppäranta and Omstedt, 1990). For the modelling of form drag etc. the reader is referred to Omstedt and Wettlaufer (1992).

3. Analytical approach

Simple analytical solutions of eqs. (1) and (2) can be derived if we only consider vertical mean properties in the system and a linear ice-water stress law. The vertically integrated momentum equations take the following form.

Ice:

$$m\frac{dU_i}{dt} = \tau_a - \tau_0 - ifmU_i; \tag{4}$$

Water:

$$M\frac{dU}{dt} = \tau_0 - \tau_b - ifMU, \tag{5}$$

where m is the ice mass per unit area ($m = \rho_i h_i$), M is the water mass per unit area ($M = \rho_w H$) and U is the vertically integrated current velocity ($U = (1/H)\int_0^H U_w\, dz$).

Introducing linear stress laws according to:

$$\tau_a = C_a U_a, \tag{6}$$

$$\tau_0 = C_0 e^{i\theta}(U_i - U), \tag{7}$$

$$\tau_b = -rU, \tag{8}$$

where U_a is the surface wind, C_a, C_0 and r are friction coefficients with dimension $[ML^{-2}T^{-1}]$ and θ is the deflection angle for the ice-water stress. It should be noticed that in general the linear drag law for sea ice is a good approximation to the quadratic law over a broad range of forcing (Martinson and Wamser, 1990). When linear models are applied one should however apply a linear air stress as well as linear ocean stresses and not mix the stress formulations with a quadratic law. The analytical solutions of eqs. (4) and (5) are given in Section 9.

Whether the ice drift and the current will amplify or damp out can be studied by examining the stationary solution in eq. (A.8) (Section 9) in some more detail. With some rearrangements the equation reads:

$$U_0 = \frac{P_0(c_2 + i\omega)}{c_1c_2 - a_1a_2 - \omega^2 + i\omega(c_1 + c_2)}. \tag{9}$$

This equation has a maximum value at $\omega = -f$. The maximum value for the ice velocity reads:

$$\frac{U_i^\infty}{U_a} = C_a\left(\frac{1}{r} + \frac{e^{-i\theta}}{C_0}\right). \tag{10}$$

The largest value thus only depends on the drag coefficients, and for constants given in Table 1 the value becomes equal to 7.8% with an angular deflection of 3.6° to the right of the wind. The corresponding extreme value for the current reads:

$$\frac{U_w^\infty}{U_a} = \frac{C_a}{r} \tag{11}$$

This extreme value now only depends on the air and bottom friction coefficients and becomes, by use of the constants given in Table 1, equal to 5.5% with zero angular deflection. For $\omega = -f$, all terms containing f in eq. (9) cancel, and the above simple equations (10) and (11) result. For $\omega \neq -f$, the corresponding expressions are more complicated and contain terms giving more dependency upon ice thickness and/or water depth.

In the case of a constant wind direction ($\omega = 0$) and an ice thickness of 0.5 m, the ice factor

Table 1. *Model constants in the analytical model*

	Constant	Value	Unit
f	Coriolis' parameter	$1.3 \cdot 10^{-4}$	s^{-1}
C_a	linear air drag coefficient	0.0164[a)]	$kg\,m^{-2}\,s^{-1}$
C_0	ice-water drag coefficient	0.7	$kg\,m^{-2}\,s^{-1}$
θ	ice-water drag angle	12	degrees
r	bottom drag coefficient	0.3	$kg\,m^{-2}\,s^{-1}$
ρ_a	air density	1.3	$kg\,m^{-3}$
ρ_i	ice density	$9 \cdot 10^2$	$kg\,m^{-3}$
ρ_w	water density	10^3	$kg\,m^{-3}$
H	water depth	80	m

[a)] $C_a = 1.3 \cdot 0.0018 \cdot 7$; this linear drag coefficient gives the same air-ice stress as the commonly used square law for $U_a = 7\ ms^{-1}$.

becomes equal to 2.3% with an ice angular deflection of $-20°$. This is in good accordance with observations from the Baltic Sea (Leppäranta and Omstedt, 1990). The corresponding values for the current factor and current angular deflection is 0.15% and $-93°$, respectively. For definition of the angles, see Fig. 1.

4. Numerical approach

Numerical solutions of eqs. (1) and (2) can be obtained if we close the equations by introducing a turbulence model. Several models for the upper layers of the ocean are available today. In the present paper, we only deal with the two-equation model, which was also applied in the study of Leppäranta and Omstedt (1990), see also Burchard and Baumert (1995) for a comparison between different turbulence models. The turbulent kinematic viscosity is calculated from the Prandtl/Kolmogorov relation:

$$\nu_T = C_\mu k^2/\varepsilon, \tag{12}$$

where C_μ is an empirical constant, k the turbulent kinetic energy and ε the dissipation rate of turbulent kinetic energy. The k and ε equations read:

$$\frac{\partial k}{\partial t} = \frac{\partial}{\partial z}\left(\frac{\nu_T}{\sigma_k}\frac{\partial k}{\partial z}\right) + \nu_T\left(\frac{\partial U_w}{\partial z}\right)^2 - \varepsilon, \tag{13}$$

$$\frac{\partial \varepsilon}{\partial t} = \frac{\partial}{\partial z}\left(\frac{\nu_T}{\sigma_\varepsilon}\frac{\partial \varepsilon}{\partial z}\right) + C_{1\varepsilon}\nu_T\frac{\varepsilon}{k}\left(\frac{\partial U_w}{\partial z}\right)^2 - C_{2\varepsilon}\frac{\varepsilon^2}{k}, \tag{14}$$

where σ_k, σ_ε, $C_{1\varepsilon}$ and $C_{2\varepsilon}$ are constants given in Table 2.

Eqs. (1), (2) and (12)–(14) form a closed system and constitute the numerical model. This set of equations, in their finite difference form, were integrated forward in time using an implicit scheme and a standard tri-diagonal matrix algorithm (Svensson, 1986). The numerical solutions were tested and found to be grid- and time-step-independent. This was achieved by a grid with 40 cells covering a depth of 80 m and a time step equal to 60 s.

5. Model calculations and results

5.1. *Ice-ocean stress laws*

In the parametrization of the ice-ocean stress we are interested in the shape of the stress versus velocity. In the analytical model given above, we assume a linear stress law, while in the numerical model the stress-velocity relation is calculated from a turbulence model. From extensive measurements in the Arctic Ocean, McPhee (1979) examined the ocean boundary layer under drifting sea ice. By identifying free ice drift periods, with ice inertial oscillations and fairly uniform wind conditions, McPhee collected a 60 days observation period from summer 1975, from which data on the upper ice-ocean boundary layer were available. The presence of inertial motions indicated that internal ice forces were small, which therefore was believed to define the best time for testing stress

Table 2. *Model constants in the numerical model*

	Constant	Value	Units
C_μ	constant in the turbulence model	0.09	
$C_{1\varepsilon}$	constant in the turbulence model	1.44	
$C_{2\varepsilon}$	constant in the turbulence model	1.92	
$C_{3\varepsilon}$	constant in the turbulence model	0.8	
σ_k	Prandtl/Schmidt number	1.4	
σ_ε	Prandtl/Schmidt number	1.3	
f	Coriolis' parameter	$1.3 \cdot 10^{-4}$	s^{-1}
ρ_a	air density	1.3	$kg\,m^{-3}$
C_d^a	air drag coefficient	$1.8 \cdot 10^{-3}$	
z_0^w	ice-water roughness length	0.05	m
z_0^b	water-bottom roughness length	10^{-4}	m
ρ_i	ice density	$9 \cdot 10^2$	$kg\,m^{-3}$
ρ_w	water density	10^3	$kg\,m^{-3}$
H	water depth	80	m

relationships, McPhee (1986). The ice-ocean stress law was assumed to be proportional to the ice drift with an arbitrary power b. The best statistical fit to the data showed a power slightly less than 2 ($b = 1.78 \pm 0.12$).

The stress-velocity relation for the models applied in the present study and the result from McPhee are illustrated in Fig. 2. The absolute values for the different models were calibrated to give the same stress corresponding to an ice speed of 0.14 m/s, or a wind speed of 7 m/s. The figure illustrates an almost complete agreement between the results from the numerical model and the data from McPhee (1979). The linear law overestimates the stress at low velocities and underestimates the stress at high velocities. The deviation from a square law dependence was discussed by McPhee (1979), where he showed that b should become equal to 1 for the classical Ekman approach with constant eddy viscosity and equal to 2 for the case in which the eddy viscosity is scaled by u_*^2/f. By introducing a wall layer close to the ice, where the eddy viscosity increases linearly, McPhee (1986) could predict the observed power relation. The wall layer with almost linearly increasing eddy viscosity close to the ice is also modelled in the present numerical model, see Leppäranta and Omstedt (1990, Fig. 11). This explains the very good agreement between the numerical model and the data in Fig. 2, supporting an ice-water stress relation with a power slightly less than 2.

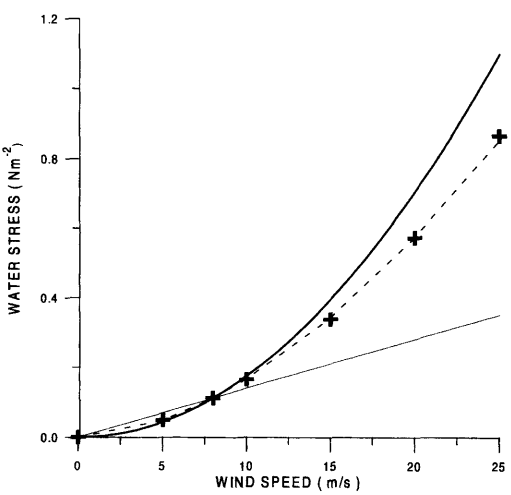

Fig. 2. Ice-ocean stress laws according to square law (thick line), linear law (thin line), McPhee (1986) (dashed line) and the numerical model (crosses).

5.2. *Stationary response during constant and periodic forcing*

In this section, we will first compare the analytical and numerical models by examining the asymptotic or stationary solutions for the case of constant winds. In Fig. 3, some results are illustrated. The figure shows that in the case of a wind speed of 7 m/s, the solutions from the two models

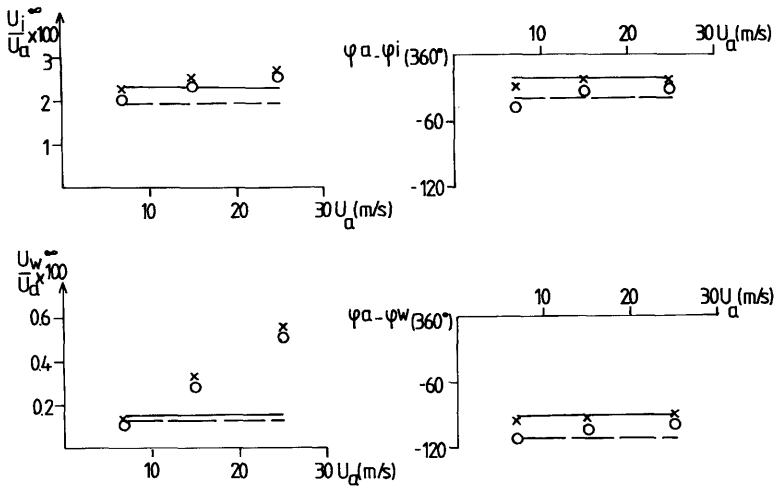

Fig. 3. Stationary solutions from the analytical and numerical models for constant winds. The analytical solutions for the case of ice thicknesses of 0.5 and 3.0 m are denoted with fully drawn and dashed lines respectively. The numerical solutions for ice thicknesses of 0.5 and 3.0 m are denoted with crosses and circles respectively.

are almost similar. This is the case we have used for the calibration of the analytical model, see discussion in the next section. By normalizing the ice drift (the ice factor) and the current speed (the current factor) with the wind speed it becomes clear that the analytical solutions are constant with changes in wind speed. The numerical solutions, which are based upon wind stresses proportional to the square of the wind speed, increase, however, with the wind speed. When the ice thickness is equal to 0.5 m, the ice factor increases from 2.3% to 2.7% when the wind speed is changing from 7 to 25 m/s. The corresponding change of current factor is from 0.15% to 0.55%. Thus the wind speed dependency is stronger for the current factor compared to the ice factor. This indicates that linear stress laws are less applicable in ocean models compared to sea ice models. For an increasing ice thickness etc., see Table 3.

Stationary solutions with periodic forcing at the inertial frequency ($\omega = -f$) are also presented in Table 3. The ice factor and the current factor in the analytical model do not show any wind or ice thickness dependency. This is in accordance with eqs. (10) and (11), which give the maximum theoretical ice and current factors. The corresponding values for the numerical model are in good agreement but show a weak wind speed dependency. Resonance conditions thus increase the ice factor from about 2 to 8%, or a factor of 4. The corresponding change of the current factor is from about 0.2 to 5, a factor of 30. This is a quite remarkable feature and illustrates that resonance conditions increase the energy more into the sea than into the ice. Energy fluxes to internal waves may in nature reduce the current factor, this has however not been dealt with in the present theory.

5.3. *Transient response during constant and periodic forcing*

The spin-up and spin-down adjustments to constant forcing are illustrated in Fig. 4. The wind speed was taken to be equal to 7 m/s during 63 days and then equal to 0 m/s, and the analytical model was calibrated towards the numerical one for this case. The calibration coefficients in the analytical model were C_0, θ and r; see Table 1. The corresponding values in the numerical model z_0^w and z_0^b, see Table 2, were taken from an earlier study when field data from the Baltic Sea were analysed (Leppäranta and Omstedt, 1990). The good agreement between the two models, with almost exactly the same stationary values, should be noticed. The main discrepancy between the models was due to the fact that the numerical model resolved the ocean in the vertical. Bottom friction thus did not reduce the inertial oscillations

Table 3. *A comparison between asymptotic solutions based upon the numerical model (N) and the analytical model (A)*

Frequency ω (s^{-1})	Ice thickness h_i (m)	Wind speed U_a (ms^{-1})	Ice factor U_i^∞/U_a (%)		Current factor U_w^∞/U_a (%)		Ice angular deflection $\phi^a - \phi^i$ (360°)		Current angular deflection $\phi^a - \phi^w$ (360°)	
			N	A	N	A	N	A	N	A
$-f$	0.5	7	7.8	7.8	5.1	5.5	0	−4	0	0
$-f$	0.5	15	8.0	7.8	5.2	5.5	0	−4	0	0
$-f$	0.5	25	8.0	7.8	5.2	5.5	0	−4	0	0
$-f$	3.0	7	7.8	7.8	5.1	5.5	0	−4	0	0
$-f$	3.0	15	8.0	7.8	5.2	5.5	0	−4	0	0
$-f$	3.0	25	8.0	7.8	5.2	5.5	0	−4	0	0
0	0.5	7	2.3	2.3	0.15	0.15	−27	−20	−95	−93
0	0.5	15	2.5	2.3	0.33	0.15	−22	−20	−93	−93
0	0.5	25	2.7	2.3	0.55	0.15	−21	−20	−91	−93
0	3.0	7	2.0	1.9	0.12	0.13	−46	−39	−114	−112
0	3.0	15	2.4	1.9	0.30	0.13	−33	−39	−103	−112
0	3.0	25	2.6	1.9	0.52	0.13	−29	−39	−98	−112

as effectively as in the case of a slab model (the analytical model). In this figure, we can notice rapid spin-up and spin-down for the ice with oscillations during many days around the stationary values. The corresponding solutions for the currents show a slower adjustment.

In Fig. 5, the spin-up and spin-down in the case of constant forcing but with different wind speeds are illustrated. In this figure, we only consider solutions from the numerical model, as the analytical model results are wind-speed-independent. Stronger winds cause larger amplitudes in the inertial oscillations, but a more rapid convergence towards the stationary values can be observed. Again the winds were constant during the first 63 days and after that equal to 0 m/s.

The model results for the case of periodic wind forcing at the inertial frequency ($\omega = -f$) are illustrated in Fig. 6. The agreement between the two models is excellent. The adjustment time is several days, but already after two days the ice factor is considerably increased, compared to the corresponding value for a constant wind, see further discussion in Section 6.

When the wind is shut off, the ice velocity in both the analytical and the numerical model rapidly adjusts to the water velocity, and the resulting inertial oscillations decay rapidly, at about the same rate for all cases. The seemingly fast spin-down of the ice velocity for the case $\omega = 0$ is thus mainly an effect of this adjustment to the very low value of the water velocity (current factors of the order 0.1–0.5%). For the case $\omega = -f$, the current factor is nearly as high as the ice factor; for values of ω outside a narrow interval around $-f$, the current factor is much lower. Obviously, when the forcing has a frequency close to $-f$, the transfer of energy to the water column is very efficient. Otherwise, rather little energy penetrates down into the water.

5.4. *Stationary response during periodic forcing*

The stationary response to periodic forcing with constant amplitude at different frequencies can most easily be analysed by examination of the particular solutions for ice and currents in the analytical model, see eqs. (A.8) and (A.10) in Section 9. The solutions are illustrated in Fig. 7, together with some calculations from the numerical model. The maximum amplitudes in the ice and current factors are quite narrow peaks at the

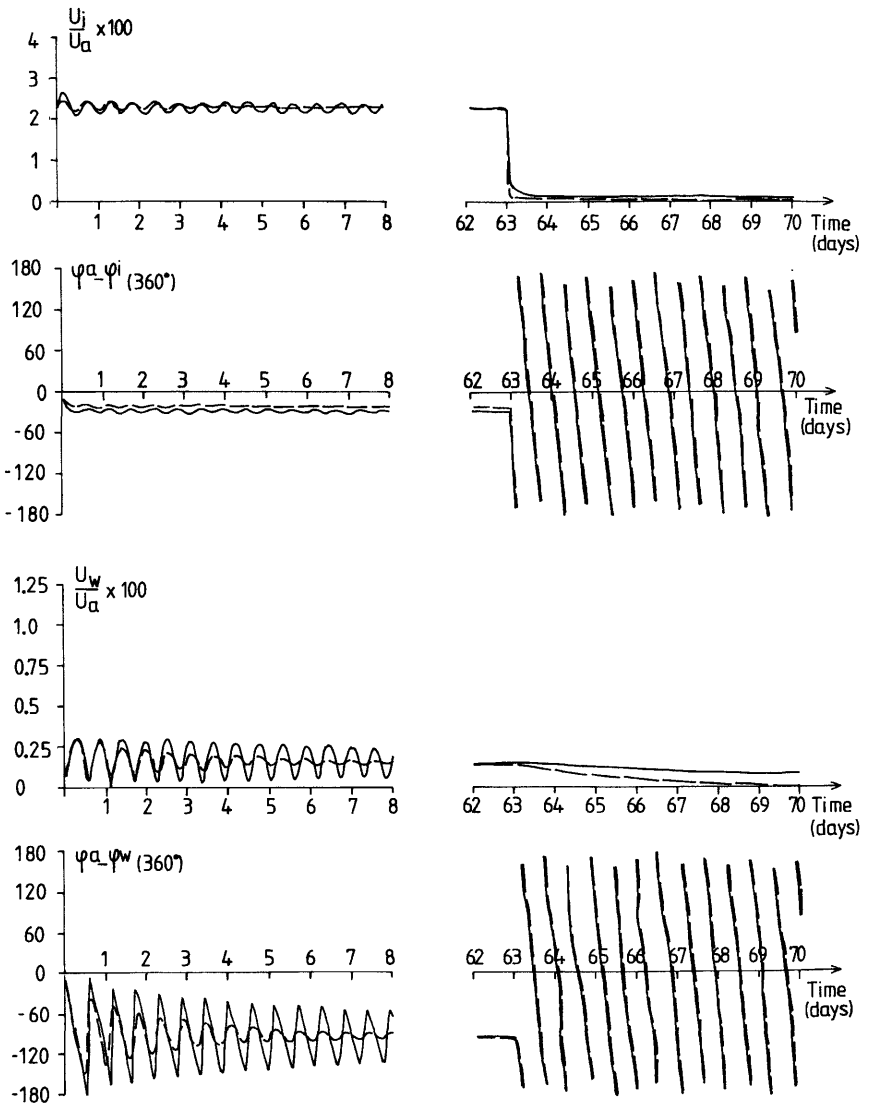

Fig. 4. Spin-up and spin-down for a constant wind speed of 7 m/s and an ice thickness of 0.5 m. The numerical and analytical solutions are denoted by fully drawn and dashed lines respectively.

inertial frequency. The damping of the current factor is almost complete for frequencies larger than $+f$ and less than $-3f$. The damping of the ice factor is less effective and also quite ice-thickness-dependent.

In the numerical model, the currents were resolved in the vertical. For comparison with the analytical model, vertical means were calculated. For more extreme changes in wind direction (frequencies outside the interval $-3f$ to $0.5f$) the difference between the wind and current directions did not reach a stable value. The reason for this was that the current in the deeper cells changed its direction with the inertial frequency $-f$, while the forcing penetrating from above had a much different frequency. The vertical mean current direction thus became poorly defined and was subject to sudden changes when the lag reached

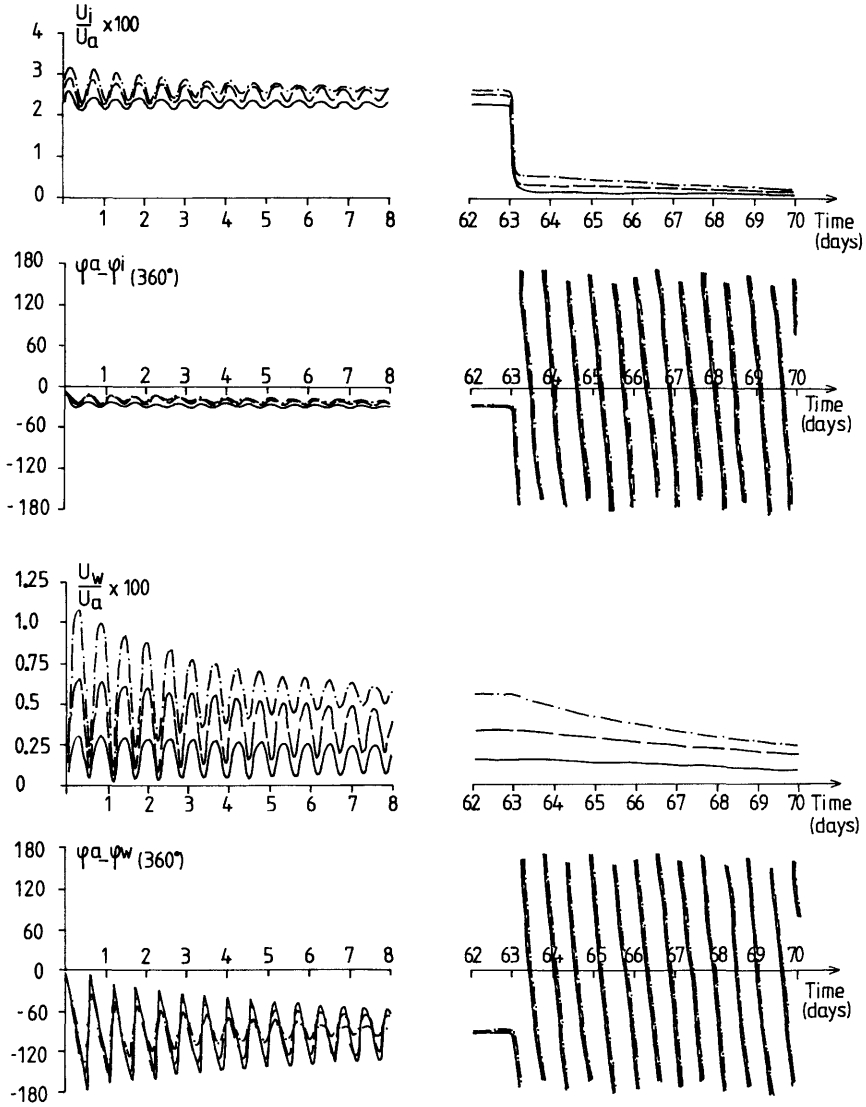

Fig. 5. Spin-up and spin-down for constant winds of 7 (full drawn lines), 15 (dashed lines) and 25 (dashed dotted lines) m/s and an ice thickness of 0.5 m. Numerical model simulations only.

values over 180°. Numerical solutions outside the interval $-3f$ to $0.5f$ were thus difficult to get and are not further dealt with.

6. Discussion

The sensitivity of the ice and current factors to changing winds have in the present work been studied only from a theoretical point of view. The applicability of some parts of the theory to observations in nature is probably of minor importance, as for example it is unrealistic to assume that the winds change direction with inertial frequency for many periods. Also in the theory we have neglected energy fluxes to internal waves and only considered damping due to bottom friction (shallow seas).

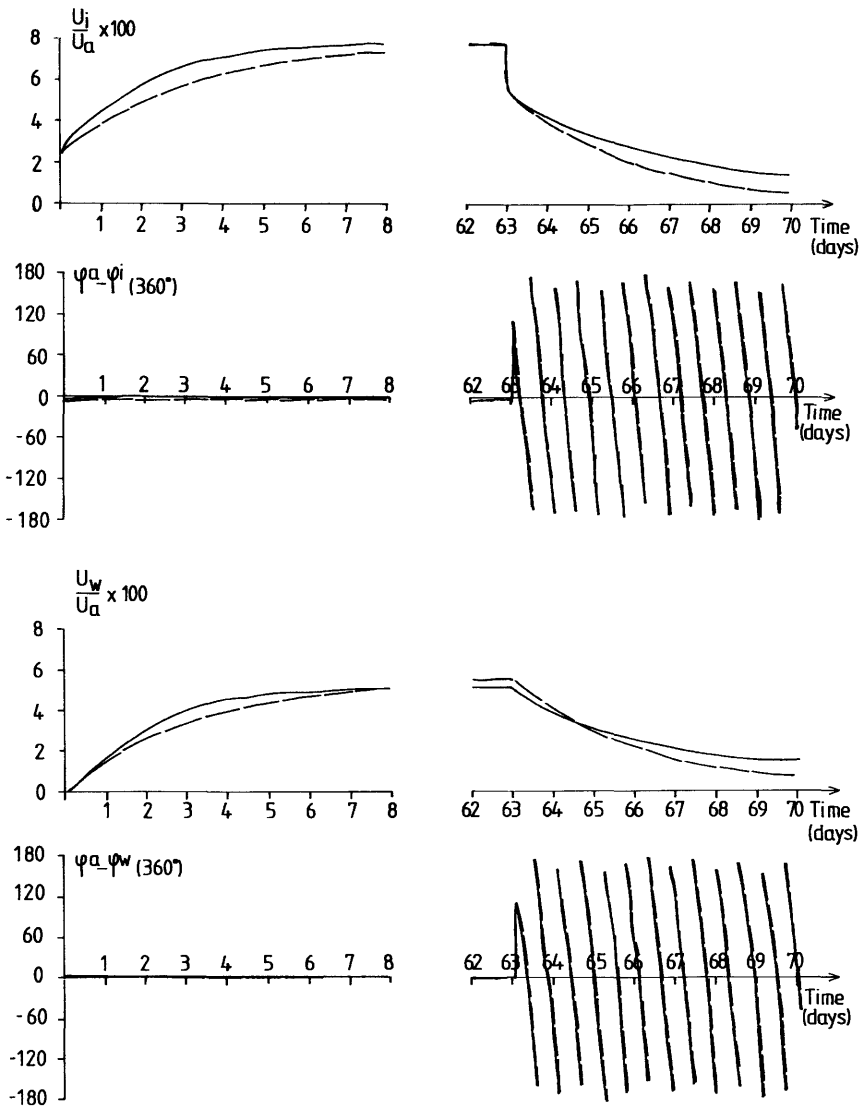

Fig. 6. Spin-up and spin-down for a periodic wind with a speed of 7 m/s and a frequency $\omega = -f$, and an ice thickness of 0.5 m. The numerical and analytical solutions are denoted with fully drawn and dashed lines respectively. Note: different scales compared to Figs. 3–5.

Observations of the oceanic response to tropical storms, with changes in wind direction, are reviewed by for example Price (1981), Shay et al. (1992) and Price et al. (1994). Based upon oceanographic observations, dramatic effects on sea surface temperatures have been observed, large temperature fluctuations in the thermocline with frequencies close to the inertial frequency, and mixed layer currents of the order of 1 m/s.

In the case of ice covered seas inertial motions have been observed particularly during summer melt periods and with inertial oscillations initiated by the passage of atmospheric fronts. The response to a changing wind with frequency close to inertial

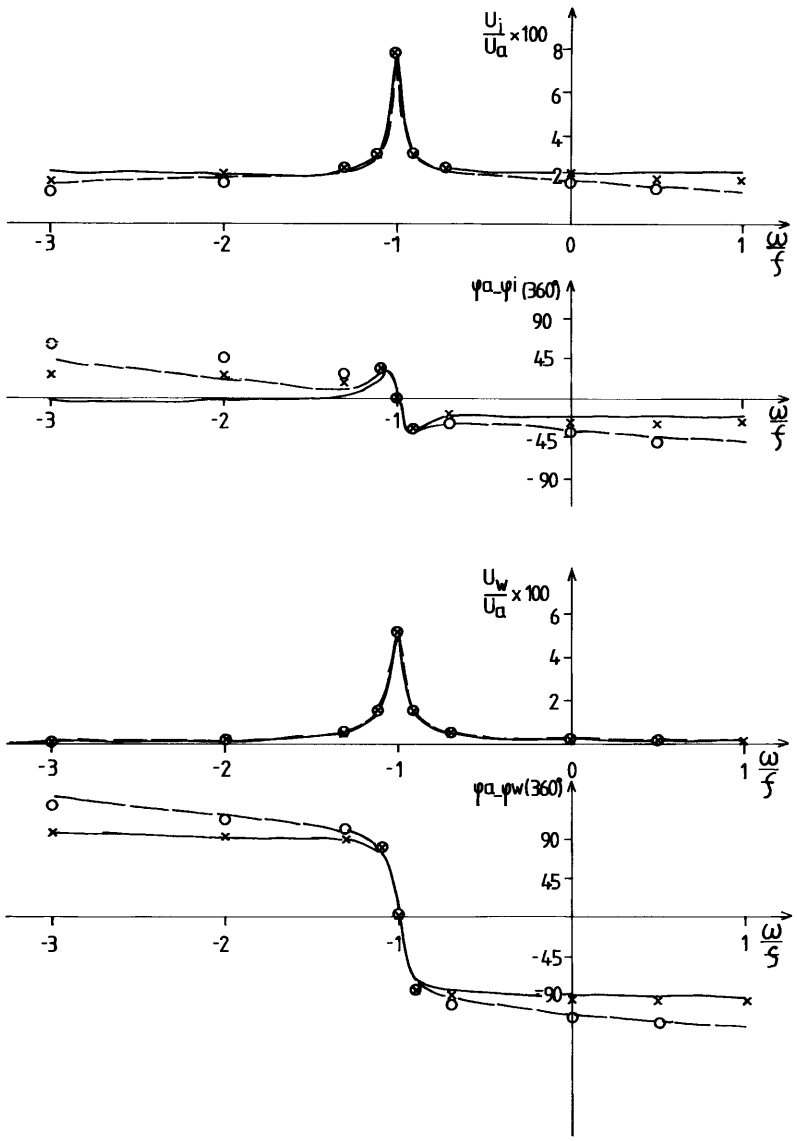

Fig. 7. Stationary solutions from the analytical and numerical models for periodic forcing of different frequencies (ω). The analytical solutions for ice thicknesses of 0.5 and 3.0 m are denoted by fully drawn and dashed lines respectively. The numerical solutions for ice thicknesses of 0.5 and 3.0 m are denoted by crosses and circles respectively.

is reanalysed in Fig. 8. As we can notice from the figure, the model calculations rather slowly approach the steady state values discussed in Section 5. Again, the steady state results in the case when $\omega = -f$ are unrealistic, as it would require a changing wind direction for many inertial periods before they are reached. However, if we only consider the increased ice and current factors for half an inertial period (about 7 h in the present calculations) we can notice that the ice and currents factors increase from zero to 3.1% and 0.5% respectively. Changing wind direction close to

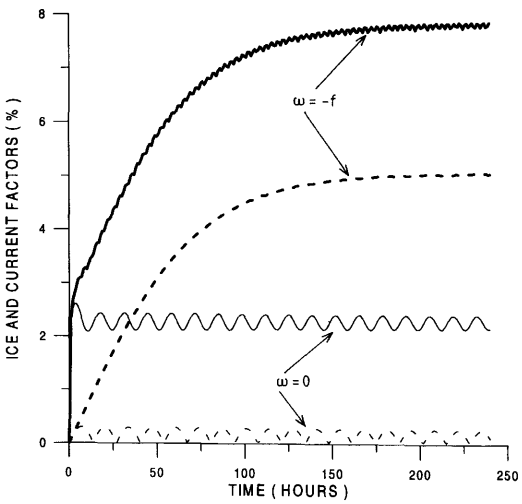

Fig. 8. Spin-up for a wind with a speed of 7 m/s and an ice thickness of 0.5 m. Two wind frequencies are illustrated $\omega = -f$ (thick lines) and $\omega = 0$ (thin lines). The fully drawn lines represent the ice factor and the dashed lines represent the current factor. Numerical model simulation only.

inertial frequencies, which is not unusual during cold front passages, could thus increase the ice and current factors considerably. From observations in the Baltic Sea we have however not been able to make observations that could support these theoretical findings. In general, deviations in ice and current factors are often claimed to be due to such features as ice thickness, form drag, roughness or atmospheric stability. In future field activities, we also need to consider the effects due to changing winds.

7. Summary and conclusions

Here, we have examined the ice-water response to changes in wind, particularly periodic forcing in shallow seas. Two models have been introduced, an analytical model based upon linear stress laws and a numerical vertically resolved model, which calculated exchange coefficients from a turbulence model and applied a square law parameterization of the wind stress formulation. The analytical model was calibrated with the numerical one. The calibration coefficients were the air friction coefficient, the ice-water drag coefficient and angle at the ice-ocean interface, and the bottom friction coefficient. The corresponding coefficients in the numerical model were taken from an earlier study where the numerical model was calibrated with field data from the Baltic Sea. By comparing the shape of the ice-ocean stresses versus ice velocity a good agreement between the numerical model and field observations from the Arctic Ocean was found. The ice-ocean response to variable winds was analysed from transient calculations with different forcing conditions.

Our conclusions may be summarized as follows:

The ice-ocean response to variable winds could be well simulated, both with an analytical and a numerical model approach. The analytical model did not capture the wind speed dependency, as linear stresses were introduced, but otherwise showed good agreement with the numerical model.

The spin-up and spin-down of the ice and current response showed a rapid adjustment for ice and a slower for currents. Strong winds adjusted the currents more rapidly than weak winds.

The maximum ice and current factors for periodic forcing were found for winds with inertial frequency ($\omega = -f$). The ice-ocean response at that frequency (stationary solution) was shown to be independent of wind speed and ice thickness but dependent on friction coefficients. For typical values used in the present study, the maximum ice and current factors were calculated to 7.8% and 5.5%, respectively. These values are however unrealistic as they would require a uniformly changing wind direction for many inertial periods.

The amplification of the ice and current factors due to winds near the inertial frequency and the damping at higher and lower frequencies was well documented in both models.

Finally, the study has demonstrated how useful it is to compare different models. From the analytical model, which was more simplified, we could get rapid solutions. From the numerical model variation in forcing conditions could be studied in more detail. For a typical run of 2000 h, a time step of 60 s and 40 grid cells in the numerical model, and a time step of 3600 s in the analytical model, the CPU time was 34 min and 2.5 s for the two models, respectively.

8. Acknowledgements

This work has partly been financed by SMHI and partly by the Swedish Natural Science Research Council. Special thanks are given to Jörgen Sahlberg for some inspiring ideas about the current response to changing winds and to one of the reviewers for valuable comments. The typing by Anneli Arkler and Gunilla Mild is also gratefully acknowledged.

9. Appendix

The analytical model

Starting from the momentum eqs. (4) and (5) and introducing linear stress laws, eqs. (6)–(8), the analytical model equations read:

$$\frac{dU_i}{dt} = -\left(\frac{C_0 e^{i\theta}}{m} + if\right) U_i + \frac{C_0 e^{i\theta}}{m} U + \frac{\tau_a}{m}, \quad (A.1)$$

$$\frac{dU}{dt} = -\left(\frac{C_0 e^{i\theta}}{M} + if + \frac{r}{M}\right) U + \frac{C_0 e^{i\theta}}{M} U_i. \quad (A.2)$$

If we now denote:

$$c_1 = \left(\frac{C_0 e^{i\theta}}{m} + if\right), \qquad a_1 = \frac{C_0 e^{i\theta}}{m}, \qquad P = \frac{\tau_a}{m},$$

$$C_2 = \frac{C_0 e^{i\theta}}{M} + if + \frac{r}{M}, \qquad a_2 = \frac{C_0 e^{i\theta}}{M},$$

the equations read:

$$\frac{dU_i}{dt} = -c_1 U_i + a_1 U + P, \quad (A.3)$$

$$\frac{dU}{dt} = -c_2 U + a_2 U_i. \quad (A.4)$$

These equations can easily be solved using the elimination method. A second-order equation is then obtained for U_i.

$$\frac{d^2U_i}{dt^2} + (c_1 + c_2)\frac{dU_i}{dt} - (a_1 a_2 - c_1 c_2)U_i = c_2 P + \frac{dP}{dt}. \quad (A.5)$$

The roots of the characteristic equation are:

$$\lambda_{1,2} = -\frac{1}{2}(c_1 + c_2) \pm \sqrt{\frac{1}{4}(c_1 - c_2)^2 + a_1 a_2}, \quad (A.6)$$

and the solution of the homogeneous case for the ice is:

$$U_i^h = A e^{\lambda_1 t} + B e^{\lambda_2 t}, \quad (A.7)$$

where A and B are constants.

To solve the general case, we need to add a particular solution to eq. (A.5). If we assume that the forcing is periodic with constant amplitude, i.e. $P(t) = P_0 e^{i\omega t}$, a particular solution can be found according to:

$$U_i^p = \frac{P_0(c_2 + i\omega) e^{i\omega t}}{\lambda_1\lambda_2 - \omega^2 - i\omega(\lambda_1 + \lambda_2)} = U_0 e^{i\omega t}, \quad (A.8)$$

where

$$P_0 = \frac{C_a U_a}{m}.$$

The general solution to eqs. (A.3) and (A.4) can now be written according to:

$$U_i = A e^{\lambda_1 t} + B e^{\lambda_2 t} + U_0 e^{i\omega t}, \quad (A.9)$$

$$U = \frac{1}{a_1}\{A(\lambda_1 + c_1) e^{\lambda_1 t} + B(\lambda_2 + c_1) e^{\lambda_2 t} + (c_1 + i\omega)U_0 e^{i\omega t} - P_0 e^{i\omega t}\}, \quad (A.10)$$

where A and B are determined by the initial conditions. If we assume no ice drift and currents at an initial time ($t = 0$), the constants read:

$$A = -B - U_0, \quad (A.11)$$

$$B = (P_0 + U_0(\lambda_1 - i\omega))/(\lambda_2 - \lambda_1). \quad (A.12)$$

Eqs. (A.8)–(A.12) form a closed system and constitute the analytical model. It should be noticed from equation (A.9), that the third term on the right side represents the stationary ice drift solution (U_i^∞) in the case of steady winds, while the first two terms represent the transient part. The first term approaches zero slowly and is negligible after 15 days. The second term approaches zero faster and becomes negligible after 2–15 h, depending on ice thickness and wind speed.

REFERENCES

Burchard, H. and Baumert, H. 1995. On the performance of a mixed-layer model based on the k-ϵ turbulence closure. *J. Geophys. Res.* **100**, C5, 8523–8540.

Ekman, V. W. 1905. On the influence of the earth's rotation on ocean currents. *Ark. Mat. Astron. Fys.* **2**, 1–53.

Gustafson, T. and Kullenberg, B. 1936. Untersuchungen von Trägheitsströmungen in der Ostsee. *Svenska Hydrogr.-Biol. Komm. Skr. Ny Ser. Hydrogr.* **13**, 1–28.

Hibler III, W. D. 1986. Ice dynamics. In: *The geophysics of sea ice* (ed. N. Untersteiner). The NATO ASI Series, B 146. New York, Plenum, 577–640.

Leppäranta, A. and Omstedt, A. 1990. Dynamic coupling of sea ice and water for an ice field with free boundaries. *Tellus* **42A**, 482–495.

Martinson, D. G. and Wamser, C. 1990. Ice drift and momentum exchange in winter Antarctic pack ice. *J. Geophys. Res.* **95**, C2, 1741–1755.

McPhee, M. G. 1978. A simulation of inertial oscillation in drifting pack ice. *Dyn. of Atm. and Oceans* **2**, 107–122.

McPhee, M. G. 1979. The effect of the oceanic boundary layer on the mean drift of pack ice: Application of a simple model. *J. Phys. Oceanogr.* **9**, 388–400.

McPhee, M. G. 1986. The upper ocean. In: *The geophysics of sea ice* (ed. N. Untersteiner). The NATO ASI Series, B146. Plenum: USA, 399–394.

Nansen, F. 1902. *Oceanography of the North Polar Basin.* The Norwegian North Polar Expedition 1893–96. Scientific Results, Vol. III, No. 9, Kristiania, Norway.

Omstedt, A. and Wettlaufer, J. S. 1992. Ice growth and oceanic heat flux: Models and measurements. *J. Geophys. Res.* **97**, (C6), 9383–9390.

Overland, J. E., Mofjelt, H. O. and Pease, C. H. 1984. Wind-driven ice drift in a shallow sea. *J. Geophys. Res.* **89**, C4, 6525–6531.

Price, J. F. 1981. Upper ocean response to hurricane. *J. Phys. Oceanogr.* **11**, 154–175.

Price, J. F., Sandford, T. B. and Forristall, G. Z. 1994. Forced stage response to a moving hurricane. *J. Phys. Oceanogr.* **24**, 233–244.

Shay, L. K., Black, P. G., Mariano, A. J., Hawkins, J. D.. and Elsberry, R. L. 1992. Upper ocean response to Hurricane Gilbert. *J. Geophys. Res.* **97**, 20227–20248.

Shirasawa, K. and Ingram, R. G. 1991. Characteristics of the turbulent oceanic boundary layer under sea ice. Part 1: A review of the ice-ocean boundary layer. *J. Marine Systems* **2**, 153–160.

Svensson, U. 1986. *PROBE: An instruction manual.* SMHI, Report Oceanography no. 10, 88 pp., SMHI, S-601 76 Norrköping, Sweden.